REIHE INFORMATIK
19/95

Gradual and Random Binarization of Gray Scale Holograms

E. Zhang, S. Noehte, C. H. Dietrich, R. Männer
Universität Mannheim
Seminargebäude A5
D-68131 Mannheim

(revised manuscript)

(Re: Manuscript No. AO 9303)

(title)

Gradual and Random Binarization of Gray-Scale Holograms

(authors)

Eryi Zhang, Steffen Noehte, Christoph H. Dietrich, and Reinhard Männer

(institution)

Chair for Computer Science V, University of Mannheim, D-68131 Mannheim, Germany

(abstract)

A new method called gradual and random binarization (GRB) to binarize gray-scale holograms, based on an iterative algorithm, is proposed. The binarization process is performed gradually and the pixels to be binarized are chosen randomly. Errors caused by this operation are spatially diffused. A comparison with other established methods based on error diffusion, direct binary search, and iterative stepwise quantization shows that the gradual and random binarization method achieves a very good compromise between computational complexity and reconstruction quality. Optical reconstructions are presented.

(text)

1. Introduction

Computer generated holograms (CGH´s) have been investigated intensively in recent years due to their wide application range and their advantages in terms of flexibility, accuracy, size, weight, and cost. Applications can be found, e.g., in optical information processing where CGH´s are used

as filters to generate a required wavefront [1], or in optical neural networks where they are used to accomplish complex synaptic interconnections [2]. CGH´s can also be used as complex optical elements [3]. Nowadays workstations provide enough computing power to generate large CGH´s. A hologram of 1024¥1024 pixels can be generated in a few minutes.

Two steps are necessary to produce CGH´s. The first step is to determine the hologram transmission that maps a given input to a desired output. In the second step, this transmission is exposed onto a photo material, e.g., a photographic plate or film, using an appropriate output device. We concentrate our work here on binary Fourier transform holograms and on the reconstruction of an intensity distribution I(x,y) in a specified region, which we call reconstruction region.

A complex signal u(x,y)=|u(x,y)|exp{jf(x,y)} of magnitude $|u(x,y)|=\sqrt{I(x,y)}$ and random phase f(x,y) is synthesized. As in experimental holography, the hologram transmission is determined by the interference pattern $|U(\mu,n)+R(\mu,n)|^2$, where $U(\mu,n)=|U(\mu,n)|\exp\{jF(\mu,n)\}=FT\{u(x,y)\}$ is the Fourier spectrum of the object, and $R(\mu,n)=\exp\{+j2p(x_0\mu+y_0n)\}$ is a plane reference wave. (x_0,y_0) determines the position of the first-order diffraction pattern in the reconstruction. In computer holography this interference pattern can be encoded as:

$$H(\mu,\nu)=\frac{|U(\mu,\nu)|\cos[\Phi(\mu,\nu)-2\pi(x_0\mu+y_0\nu)]-Bs}{1-Bs} \qquad (1)$$

where U(μ,n) is normalized to 1, Bs=min{|U(μ,n)|cos[F(μ,n)-2¹(x₀μ+y₀n)]} is a bias factor that ensures 0²H(μ,n)²1. Note that the values (x,y) and (μ,n) are all discrete values of the form (xdx,ydy) and (μdμ,ndn), and dxdμ, dydn fulfill the sampling theorem. Thus, pixels are indexed by (x,y) and (μ,n) respectively.

The hologram distribution (1) is analog valued. The production of the corresponding hologram is normally difficult since photo materials as well as output devices usually suffer from nonlinearities. Besides, it is required that the output device is able to expose gray values. These problems are avoided in binary holograms having only two values. The production and the reproduction of

binary holograms is especially simple [4]. For exposure even plotters or laser printers can be used [5]. Additionally, binary holograms have lower noise sensitivity [6]. However, one has to take care of the binarization error, because this error can cause enormous errors in the reconstruction with respect to the original object. Many different methods have been proposed to minimize this error. They can be divided into two groups: noniterative methods and iterative methods. Hard-clipping and error diffusion [7-12] belong to the former, whereas direct binary search [13-15] and iterative stepwise quantization [16,17] belong to the latter. The new method proposed here, called gradual and random binarization (GRB) of gray-scale holograms, also belongs to the latter. It binarizes gray-scale holograms gradually and randomly, based on an iterative algorithm.

For reconstruction a common Fourier transform geometry is used, that is, the produced binary hologram is located at the front focal plane of the system and illuminated by a collimated wave parallel to the optical axis. The reconstruction appears at the back focal plane. It contains the ±1st order, i.e., the original signal $u(x-x_0,y-y_0)$ and its conjugate $u^*[-(x+x_0), -(y+y_0)]$, the 0th order, i.e., the dc peak in the center, and higher orders.

The following two sections (section 2 and section 3) describe in detail the new method and the binary holograms generated by it. A comparison with other methods is done in section 4. Optical reconstructions are presented in section 5 which is followed by conclusions (section 6).

2. Iterative algorithm and constraints

Iterative algorithms for the computation of holograms consist generally of the following steps [18,19]:

Algorithm 0:

i) Fourier transform the original signal $u(x,y)=|u(x,y)|\exp\{jf(x,y)\}$ into $U_1(\mu,n)$:

$$U_1(\mu,n)=FT\{u(x,y)\}.$$

ii) Encode the complex spectrum $U_k(\mu,n)$ into the hologram $H_k(\mu,n)$ for the k-th iterative cycle. Here C denotes the encoding, e.g., of Eq. (1):

$H_k(\mu,n)=C\{U_k(\mu,n)\}$, k=1, 2, 3, ...

iii) Impose the constraints L in the hologram domain:

$$H_k(\mu,n) \xrightarrow{L} H'_k(\mu,n).$$

iv) Inverse Fourier transform $H'_k(\mu,n)$ into $h'_k(x,y)$ that contains the signal u(x,y):

$$h'_k(x,y)=I\,F\,T\{H'_k(\mu,n)\}.$$

v) Impose the constraints l in the object domain:

$$h'_k(x,y) \xrightarrow{\ell} h_{k+1}(x,y).$$

vi) Fourier transform $h_{k+1}(x,y)$ into $U_{k+1}(\mu,n)$. Go to ii).

The constraints imposed in step iii) and step v) depend on the requirements to the hologram and to the reconstruction.

Steps i)-vi) are repeated until the signal contained in $h'_k(x,y)$ of step iv), which is reconstructed by $H'_k(\mu,n)$, has the required accuracy.

GRB uses such an iterative algorithm for the generation of binary holograms. The produced binary hologram should reconstruct the original signal |u(x,y)| in the reconstruction region as well as possible. We choose the first-order diffraction pattern in the reconstruction as the reconstruction region. The constraints in algorithm 0 are therefore determined as follows: The constraint L in the hologram domain is a threshold that transforms the gray valued hologram into a binary one. The constraint l in the object domain is a replacement, i.e., the reconstructed magnitude in the reconstruction region is replaced by the original one if both are different. Without loss of generality we assume that the hologram has N¥N pixels and the reconstruction region w has M¥M (0<M<N) pixels.

To assess the reconstruction quality quantitatively, we use the Mean Square Error (MSE). Suppose f_{xy} to be the original signal, g_{xy} to be the reconstruction of the hologram, then the MSE is computed by

$$MSE=\frac{1}{M^2}\sum_{xy\in w}\left|\frac{f_{xy}-\bar{f}}{\sigma_f}-\frac{g_{xy}-\bar{g}}{\sigma_g}\right|^2$$

where $\bar{f}=\frac{1}{M^2}\sum_{xy\in w}f_{xy}$, $\bar{g}=\frac{1}{M^2}\sum_{xy\in w}g_{xy}$, $\sigma_f^2=\frac{1}{M^2}\sum_{xy\in w}\left|f_{xy}-\bar{f}\right|^2$, $\sigma_g^2=\frac{1}{M^2}\sum_{xy\in w}\left|g_{xy}-\bar{g}\right|^2$.

The sum extends over to the entire region w. Note that the MSE is independent of the actual value of g and any additive constant.

Thus, algorithm 0 can be rewritten more detailed in the following fashion:

Algorithm 1:

i) Fourier transform $u(x,y)=|u(x,y)|\exp\{jf(x,y)\}$ into $U_1(\mu,n)$:

$$U_1(\mu,n)=F\,T\,\{u(x,y)\}.$$

ii) Encode $U_k(\mu,n)$ into $H_k(\mu,n)$ by Eq. (1) for the k-th iterative cycle, k=1, 2, ….

iii) Impose the constraint on the hologram $H_k(\mu,n)$

$$H'_k(\mu,\nu)=\begin{cases}0 & \text{if } H_k(\mu,\nu)<T_{threshold}\\ 1 & \text{otherwise}\end{cases}$$

iv) Inverse Fourier transform $H'_k(\mu,n)$ into $h'_k(x,y)$:

$$h'_k(x,y)=I\,F\,T\,\{H'_k(\mu,n)\}.$$

v) Calculate MSE of $|h'_k(x,y)|$ in region w in respect to the original signal $|u(x,y)|$. If it is not sufficiently smaller than in the last cycle, terminate the iteration; else impose the constraint of the object domain: correct pixel values of $|h'_k(x,y)|$ in region w to form $h_{k+1}(x,y)$:

$$|h_{k+1}(x,y)|=\begin{cases}|u(x,y)|/c_k & \text{if } |h'_k(x,y)|\neq|u(x,y)|/c_k\\ |h'_k(x,y)| & \text{otherwise}\end{cases}$$

where c_k is a scaling factor calculated by:

$$c_k=\frac{\sum_{(x,y)\in w}|u(x,y)||h'_k(x,y)|}{\sum_{(x,y)\in w}|h'_k(x,y)|^2}$$

vi) Fourier transform $h_{k+1}(x,y)$ into $U_{k+1}(\mu,n)$. Go to ii).

Intuitively one could expect to obtain an improved reconstruction of $H'_k(\mu,n)$ by repeating steps ii)-vi). However, this is not the case. Because the threshold in step iii) of algorithm 1 is applied to all hologram pixels, the algorithm converges to an unsatisfactory solution and stagnates there [16]. To avoid the stagnation, Wyrowski [16] proposed an iterative stepwise quantization method based on the gray-value distribution of the hologram. In his method, two variable thresholds are used in step iii) instead of a constant threshold for all the pixels. At the beginning, Threshold 1 is set to 0, whereas Threshold 2 is set to 1. Then Threshold 1 is increased, and Threshold 2 is decreased by a step. Pixels having values below Threshold 1 are set to zero, and pixels having values above Threshold 2 are set to 1. Other pixels having values between Threshold 1 and Threshold 2 are unchanged. The algorithm is iteratively performed for these two thresholds until the MSE does not longer decrease. Then new thresholds are constructed, i.e., Threshold 1 is increased, and Threshold 2 is decreased by another step, and the algorithm is started again. This action is carried out step by step until the two thresholds become equal. Using this method an improved reconstruction with smaller MSE (see section 4) has been achieved. However, this algorithm cannot diffuse the binarization error effectively, because normally a hologram is locally correlated. That is to say, there are always regions in which all pixels have values below Threshold 1 or above Threshold 2, and they are regionally binarized. Our method described in the next section overcomes this drawback by gradually increasing the number of binarized pixels which are chosen randomly on the hologram.

3. The GRB algorithm

Starting from an analog hologram $H(\mu,n)$ described by Eq. (1), and its reconstruction $h(x,y)$ containing $u(x,y)$ in region w, a Fourier transform pair $H(\mu,n)\acute{}h(x,y)$ is constructed. The constraint imposed in step iii) of algorithm 1 is decomposed into two sub-constraints, namely the number of pixels to be binarized and the choice of those pixels for the binarization. Therefore, the GRB algorithm is realized in two nested iterations: the outer loop determines how many pixels are binarized, and the inner loop chooses those pixels randomly and binarizes them. The number of

binarized pixels increases gradually with each outer iteration. Fig. 1 is the flow chart of the GRB algorithm, where the outer loop is indexed by i and the inner loop by k.

(Figure 1)

In the flow chart of Fig. 1, the following two terms have been defined:

i-th iteration: one outer loop with the i-th constraint that N^2/S_i pixels should be binarized. i=1, 2, 3, ..., I.

k-th iterative cycle: one inner loop to binarize N^2/S_i pixels. k=1, 2, 3, ..., K.

In the i-th iteration, N^2/S_i pixels in the hologram should be binarized, where S_i is an integer ($S_i << N^2$). To determine which pixels are processed in each iterative cycle k (k=1, 2, ..., K) of this iteration, N^2/S_i pseudo-random numbers between 0 and N^2-1 are generated as access addresses. It seems as if the hologram were randomly divided into N^2/S_i sub-holograms, each having S_i pixels and in which only one pixel were binarized. This operation is carried out until the MSE no longer decreases significantly. Then the (i+1)-th iteration is started with the constraint that N^2/S_{i+1} ($S_{i+1} < S_i$) pixels should be binarized.

The binarization of pixels in the gray-scale hologram introduces an error with respect to the gray-scale hologram. We call this error binarization error in the hologram. It leads to errors in the reconstruction, which we call binarization error in the reconstruction. If an iterative cycle is performed-binarization of hologram pixels, simulation of the reconstruction, replacement of pixel values in the reconstruction region, and generation of a new hologram-the error in the hologram is spread out [20]. We say the binarization error in the hologram is spatially diffused. After several iterative cycles, the binarization error in the reconstruction will be distributed to the area outside of the reconstruction region. In this way, an improved reconstruction in the reconstruction region

will be achieved. Gradual binarization avoids the stagnation of the algorithm; random binarization reduces the likelihood of local error clustering.

To speed up convergence, we select the parameters S_1, S_2, …, S_i, …, S_I to be a geometrical series of (1/2) and $S_1=S$, $S_I=1$. Thus we have altogether $I=1+\log_2 S$ iterations to accomplish. The constraints for these iterations are the binarization of pixels N^2/S, $2N^2/S$, ..., and N^2. The number of iterative cycles in each iteration differs from iteration to iteration, but we limit this number to be not larger than the number S, as a compromise between error reduction in each iteration and computation time. In practice, we can choose S=16 or S=8.

The example given below shows how the algorithm works and how the binarization errors are diffused to the neighbors. The object to be reconstructed is the capital letter 'F', represented by 30¥32 pixels of three gray values. It is located at the center of a 128¥128 zero array as shown in Fig. 2(a). Random phase is used with the amplitude to generate its gray-scale hologram. The hologram coded by Eq. (1) is shown in Fig. 2(b) with $(x_0,y_0)=(32,32)$.

(Figure 2)

To binarize the gray-scale hologram (256 gray values) of Fig. 2(b), we choose S=8. The reconstruction region w has the same size as that of the original object. The threshold value for the binarization is 0.5. Altogether $I=1+\log_2 S=4$ iterations are required, namely in the first iteration 2048 pixels are binarized, in the second 4096 pixels, in the third 8192 pixels, and in the forth 16384 pixels (due to the random selection of pixels, a pixel may be binarized more than once. This implies the number of actually binarized pixels is smaller than the number given above). In each iteration, the k-th iterative cycle ($k^2S=8$) is performed provided that the reduction of the MSE in the last two iterative cycles is large enough, here larger than 0.001, i.e. d=0.001. Fig. 3(a), 3(b), 3(c), 3(d) and 3(e) show the changes of the hologram after performing the binarization iterations; Fig. 3(a'), 3(b'), 3(c'), 3(d') and 3(e') are their gray-value distribution.

(Figure 3)

In the first iteration (i=1 and S_1=8), N^2/S_1=2048 pixels were binarized. Pseudo-random addresses determined which pixels are binarized. After performing the first iterative cycle (k=1) of this iteration (i=1), the MSE caused by the binarization of 2048 pixels was 0.05354. It was reduced by the subsequent iterative cycles (k=2, 3, ..., see Fig. 4), i.e., again 2048 pixels were randomly binarized. At the end of the first iteration (i=1), MSE was reduced to 0.02586, then the reduction became too slow. The second iteration with i=2 and S_2=4 was started. In this iteration (i=2) N^2/S_2=4096 pixels were binarized, etc.. Fig. 4 shows how the MSE changed during each iteration and with the iterations (i=1, 2, 3, 4). Table I lists their related values.

(Figure 4)

(Table I)

After the last iteration (i=4, S_4=1), the threshold was applied to all pixels to generate the final binary hologram. Fig. 5(a) shows this hologram. Its computer simulated reconstruction is given by Fig. 5(b) with MSE=1.80¥10^{-2}. The diffraction efficiency h=6.17%.

(Figure 5)

4. Comparison with established methods

To estimate the performance and the efficiency of the GRB algorithm, it has been compared with some established methods. The comparison focuses mainly onto two aspects: The computational

complexity to generate a binary hologram and the reconstruction quality in region w produced by such a hologram. As object we still take the example of section 3, capital letter 'F'. All parameters remain unchanged. The following methods are considered:

- Hard clipping.
- Error diffusion.
- Direct binary search.
- Iterative stepwise quantization.
- Gradual and random binarization (GRB).

Hard clipping is the simplest and the fastest method among the five methods considered. It scans the gray-scale hologram and binarizes it using a constant threshold. If N is the size of the hologram, the complexity of this algorithm is O(N) (the time needed to generate the gray-scale hologram is not taken into account). The reconstruction from such a binary hologram consists of the desired object and noise within and around the object. Fig. 6(a) shows the binarized hologram, Fig. 6(b) its computer simulated reconstruction with MSE=9.78¥10^{-2}. The diffraction efficiency h=8.97%.

(Figure 6)

Error diffusion method [7] was originally developed for displaying images. It has been later introduced into holographic applications [8]. The algorithm works sequentially, i.e., it processes input data line by line, pixel by pixel. The basic concept can be described as follows: The first pixel of the gray-scale hologram H(μ,n), H(0,0), is compared with a given threshold T. If H(0,0)³T, the output $H_{out}(0,0)$ is set to 1, otherwise to 0. The error $E(0,0)=H_{out}(0,0)-H(0,0)$ caused by this operation is diffused to other unprocessed pixels which are given the new value $H'(\mu,n)=H(\mu,n)-W_{\mu n}E(0,0)$ at location (μ,n), where $W_{\mu n}$ are diffusion coefficients. Modifications of this algorithm [8-12] use the same general scheme and differ mainly in the number and relative

positions of pixels included in the error diffusion. We use the method proposed by Severin Weissbach and Frank Wyrowski [12]. This algorithm determines the diffusion weights dependent on the location of the reconstruction region, and results in a zero error there. The complexity of this algorithm is O(N) too, N is the size of the hologram. Fig. 7(a) shows the generated binary hologram, Fig. 7(b) its simulated reconstruction with MSE=5.04¥10^{-2} and h=1.09%.

(Figure 7)

Direct binary search [13-15] is based on an iterative procedure to minimize a given error criterion. It manipulates the binary state of individual pixels of the hologram directly by monitoring the effect on the reconstruction region: the randomly generated initial binary hologram is scanned, and the transmission values are inverted one by one. After each inversion, the MSE in the reconstruction region is computed. If it has decreased, the inversion is retained; otherwise, the pixel is restored to its previous state. The algorithm is terminated when no inversions are retained during an entire iteration. The complexity of this algorithm is $O(N^{7/4}[\log_2 N]^{3/4})$, where N is the size of the hologram. The binary hologram generated using this method and its computed reconstruction are shown in Fig. 8(a) and Fig. 8(b) with MSE=1.40¥10^{-2} and h=3.97%. Here the algorithm is terminated when MSE²1.40¥10^{-2}.

(Figure 8)

Iterative stepwise quantization proposed by Wyrowski [16] is also based on an iterative algorithm (see section 2). A stepwise quantization based on the gray-value distribution of the hologram results in an improved convergence. As an example the binary hologram generated using this method and its computed reconstruction are given in Fig. 9(a) and Fig. 9(b). The complexity of this algorithm is $O(N\log_2 N)$, where N is the size of the hologram. The simulated reconstruction shows MSE=2.79¥10^{-2}, h=6.45%.

(Figure 9)

Gradual and random binarization (GRB) has been described in section 3. The generated binary hologram and its computed reconstruction have been given in Fig. 5(a) and Fig. 5(b). The complexity of this algorithm is $O(N\log_2 N)$ too, where N is the size of the hologram. Here MSE=1.80¥10^{-2}, h=6.17%.

Table II summarizes these results.

(Table II)

It has been shown that the direct binary search hologram achieved the best reconstruction quality. However, the required computing power is in many practical cases too large. Gradual and random binarization (GRB) achieved a very good compromise between computational complexity and the reconstruction quality. This result can be seen qualitatively by comparing computed reconstructions, e.g. Fig. 9(b) and Fig. 5(b). Fig. 9(b) is the computed reconstruction from the hologram Fig. 9(a) generated by the stepwise quantization method, and Fig. 5(b) from the hologram Fig. 5(a) generated by the GRB method. Clearly, for the stepwise quantization method errors in the reconstruction are mainly distributed to the area around the reconstruction region, whereas for the GRB method errors are uniformly distributed to the entire reconstruction plane outside of the reconstruction region. That is, the GRB algorithm distributes binarization errors more efficiently than the stepwise quantization method.

5. Optical reconstructions

The object to be reconstructed is the emblem of the University of Mannheim with 250¥340 pixels as shown in Fig. 10. It was centered on a 1024¥1024 array of zeros. Random phase was assigned to it. The reference wave was $\exp\{+j2^{1}(x_0\mu+y_0 n)\}$ with $(x_0,y_0)=(256, 256)$. Thus the object, the twin, and the DC peak were seen in the reconstruction. For comparison two binary holograms were produced. One was generated by iterative stepwise quantization, and the other by gradual and random binarization (GRB). A photo-printer with resolution of 1625 dpi was used to expose the calculated binary holograms onto a film of size 16¥16 mm^2. After chemical processing, the binary amplitude holograms were obtained. A He-Ne laser of wave length $l=0.6328\mu m$ was used for the reconstruction. Fig. 11 and Fig. 12 show the optical results.

(Figure 10)

(Figure 11)

(Figure 12)

During the optical reconstruction the diffraction efficiency was measured. The hologram was illuminated by a circular laser beam (Ø=11.6 mm). A photo power meter with a circular aperture of diameter 12 mm was used to measure the energy in the first diffraction order. The measured value is actually summed over the circular aperture of the photo power meter which is normally larger than the non-circular reconstruction region. The absorption of the holographic film and the imaging lens must also be taken into consideration.

The measured values listed in the column h' of Table III have shown a good agreement of the experimentally generated data with the computer simulations. Computer calculated MSE and h

are also listed in Table III. Both the computer simulation and the optical reconstruction have shown that the hologram generated by the method proposed here is of high quality.

(Table III)

6. Conclusions

A new method to binarize gray-scale holograms, based on an iterative algorithm, was proposed. Using this method an optimized binary hologram was generated and its optical reconstruction was demonstrated. Since pixels in the gray-scale hologram are introduced gradually and binarized randomly, the stagnation of the algorithm was avoided, and a more efficient diffusion of binarization errors was achieved [20], which results in an improved convergence. Compared with other established methods, GRB has shown a more satisfactory reconstruction at less computational demands. More tests have been done. They show that the gradual and random binarization method can always reduce errors in the reconstruction region. The error reduction degree is tightly related to the size of the reconstruction region. In this sense, this algorithm is robust.

Although the binarization method described is considered here for Fourier transform holograms only, it is possible to extend it to generate any other kind of binary holograms. Owing to the limitation of space, the theoretical foundation of this method will not be dealt with here, but in [20].

References

[1] Frank Wyrowski and Olof Bryngdahl, "Digital holography as part of diffractive optics", Rep. Prog. Phys. (1991) pp. 1481-1571.

[2] Paul E. Keller and Arthur F. Gmitro, "Design and analysis of fixed planar holographic interconnects for optical neural networks", Applied Optics, Vol. 31, No. 26 (1992) pp. 5517-5526.

[3] N. Davidson, A. A. Friesem, and E. Hasman, "Holographic axilens: high resolution and long focal depth", Optics Letters, Vol. 16, No. 7 (1991) pp. 523-525.

[4] Wilfrid B. Veldkamp and Thomas J. McHugh, "Binary Optics", Scientific American (1992) pp. 92-97.

[5] Andrew J. Lee and David P. Casasent, "Computer generated hologram recording using a laser printer", Applied Optics, Vol. 26, No. 1 (1987) pp. 136-138.

[6] T. C. Strand "Signal/noise in analog and binary holograms", Opt. Eng. 13 (1974) pp. 219-227.

[7] R. W. Floyd and L. Steinberg, "An adaptive algorithm for spatial grayscale", Proc. Soc. Inf. Disp., Vol. 12 (1976) pp. 55-77.

[8] Richard Hauck and Olof Bryngdahl, "Computer-generated holograms with pulse-density modulation", J. Opt. Soc. Am. A, Vol. 1, No. 1 (1984) pp. 5-10.

[9] S. Weissbach, F. Wyrowski and O. Bryngdahl, "Quantization noise in pulse density modulated holograms", Optics Communications, Vol. 67, No. 3 (1988) pp. 167-171.

[10] Etienne Barnard, "Optimal error diffusion for computer-generated holograms", J. Opt. Soc. Am. A, Vol. 5, No. 11 (1988) pp. 1803-1871.

[11] Reiner Eschbach, "Comparison of error diffusion methods for computer-generated holograms", Applied Optics, Vol. 30, No. 26 (1991) pp. 3702-3710.

[12] Severin Weissbach and Frank Wyrowski, "Error diffusion procedure: theory and applications in optical signal processing", Applied Optics, Vol. 31, No. 14 (1992) pp. 2518-2534.

[13] Michael A. Seldowitz, Jan P. Allebach, and Donald W. Sweeney, "Synthesis of digital holograms by direct binary search", Applied Optics, Vol. 26, No. 14 (1987) pp. 2788-2798.

[14] Brian K. Jennison, Jan P. Allebach and Donald W. Sweeney, "Efficient design of direct-binary-search computer-generated holograms", J. Opt. Soc. Am. A, Vol. 8, No. 4 (1991) pp. 652-660.

[15] Myung Soo Kim and Clark C. Guest, "Block-quantized binary-phase holograms for optical interconnection", Applied Optics, Vol. 32, No. 5 (1993) pp. 678-683.

[16] Frank Wyrowski, "Iterative quantization of digital amplitude holograms", Applied Optics, Vol. 28, No. 18 (1989) pp. 3864-3869.

[17] Chien-Hsion Wu, Chia-Lun Chen, and M. A. Fiddy, "Iterative procedure for improved computer-generated-hologram reconstruction", Applied Optics, Vol. 32, No. 26 (1993) pp. 5135-5140.

[18] J. R. Fienup, "Phase retrieval algorithms: a comparison", Applied Optics, Vol. 21, No. 15 (1982) pp. 2758-2769.

[19] R. W. Gerchberg and W. O. Saxton, "A Practical Algorithm for the Determination of Phase from Image and Diffraction Plane Pictures", Optik, Vol. 35, No. 2 (1972) pp. 237-246.

[20] Eryi Zhang, Jürgen Hesser, Christoph H. Dietrich, Steffen Noehte, Reinhard Männer, "Mathematical Analysis of Computer Generated Binary Fourier Transform Holograms", submitted to J. Opt. Soc. Am. (1995).

(List of figure captions)

Fig. 1. Flow chart of the gradual and random binarization algorithm (GRB).

Fig. 2. Object (letter 'F') with three gray values (a) and its gray-scale hologram (b) (256 gray values).

Fig. 3. Illustration of the binarization process. Partly binarized holograms for S_1=8, S_2=4, S_3=2, and S_4=1 are shown left (b)-(e), their gray-value distribution right (b')-(e'). (a) shows the original gray-scale hologram, (a') its histogram.

Fig. 4. MSE changes with iterative cycles k (1-7, 8-14, 15-19, and 20-22) in each iteration, and with iterations i (1, 2, 3, 4).

Fig. 5. Binary hologram generated by the GRB method proposed here (a) and its computer simulated reconstruction (b).

Fig. 6. Binary hologram generated by hard clipping (a) and its computed reconstruction (b).

Fig. 7. Binary hologram generated by error diffusion (a) and its computed reconstruction (b).

Fig. 8. Binary hologram generated by direct binary search (a) and its computed reconstruction (b).

Fig. 9. Binary hologram generated by iterative stepwise quantization (a) and its computed reconstruction (b).

Fig. 10. The emblem of the University of Mannheim as object.

Fig. 11. Optical reconstruction of the binary hologram generated by iterative stepwise quantization.

Fig. 12. Optical reconstruction of the binary hologram generated by gradual and random binarization (GRB).

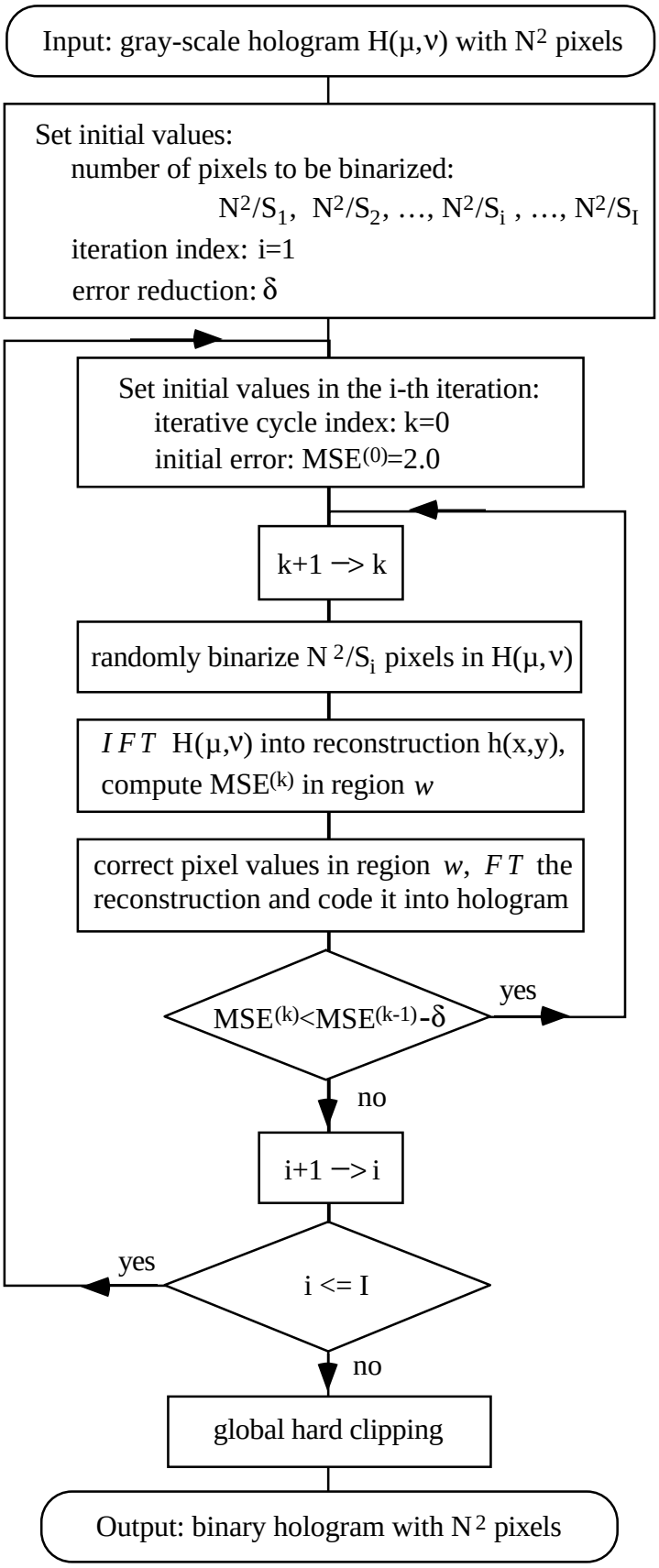

Fig. 1. Flow chart of the gradual and random binarization algorithm (GRB).

(a)

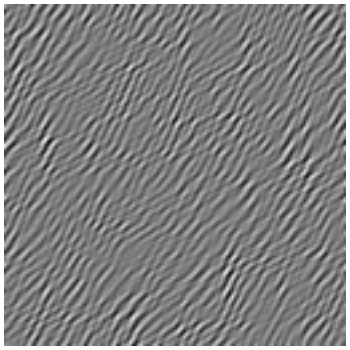

(b)

Fig. 2. Object (letter 'F') with three gray values (a) and its gray-scale hologram (b) (256 gray values).

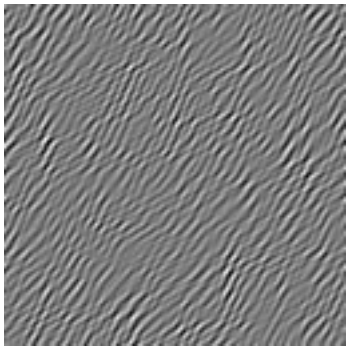

(a)

(a')

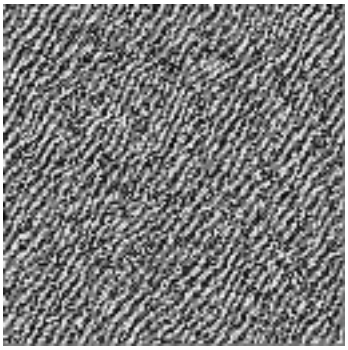

(b)

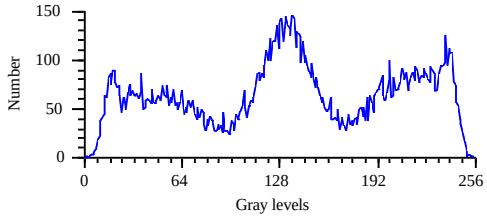

(b')

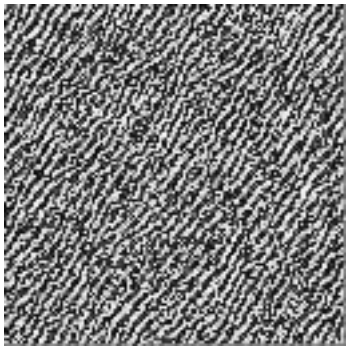

(c)

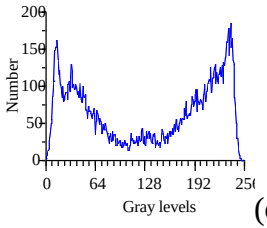

(c')

(**Fig. 3.** Illustration of the binarization process. To be continued)

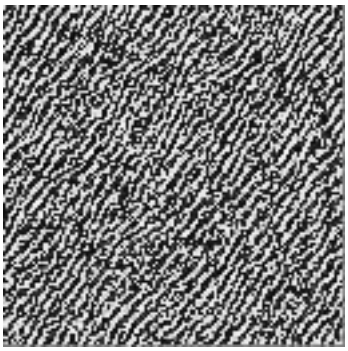

(d)

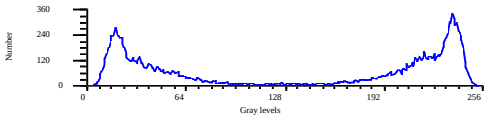

(d')

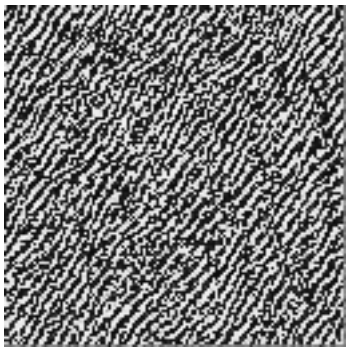

(e)

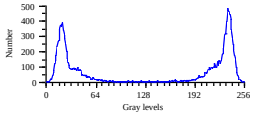

(e')

Fig. 3 (continued). Illustration of the binarization process. Partly binarized holograms for S_1=8, S_2=4, S_3=2, and S_4=1 are shown left (b)-(e), their gray-value distribution right (b')-(e'). (a) shows the original gray-scale hologram, (a') its histogram.

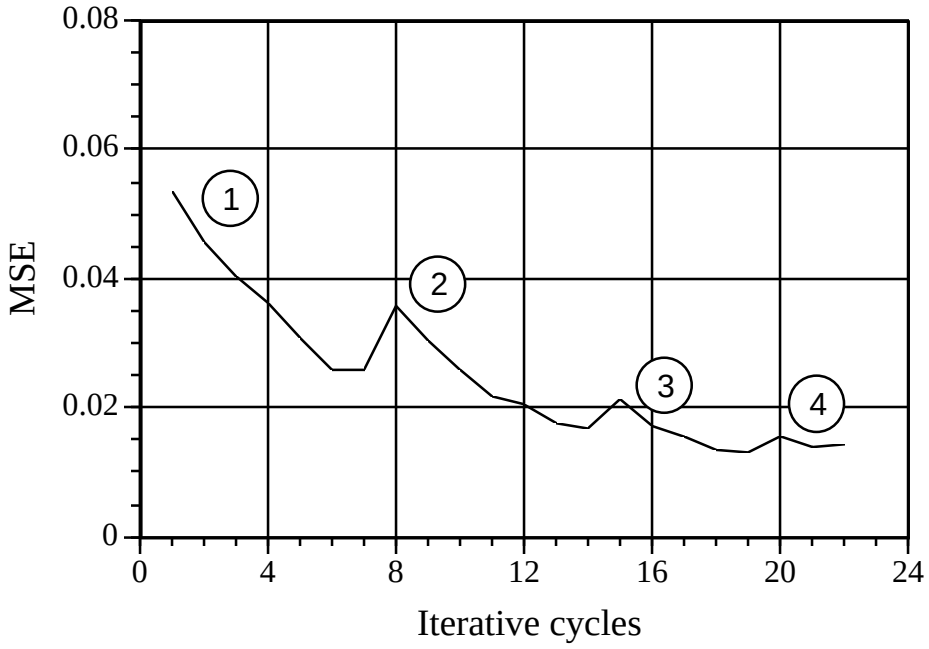

Fig. 4. MSE changes with iterative cycles k (1-7, 8-14, 15-19, and 20-22) in each iteration, and with iterations i (1, 2, 3, 4).

(a)

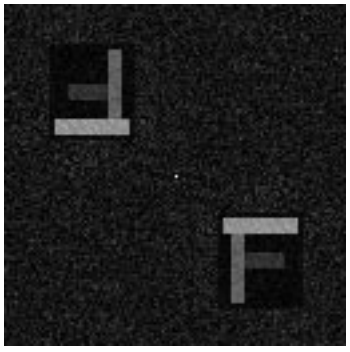

(b)

Fig. 5. Binary hologram generated by the GRB method proposed here (a) and its computer simulated reconstruction (b).

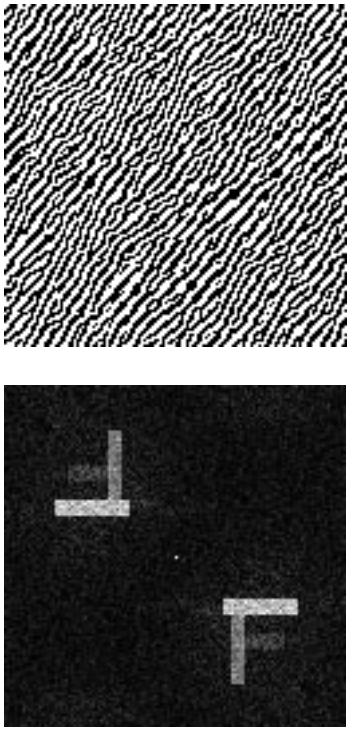

Fig. 6. Binary hologram generated by hard clipping (a) and its computed reconstruction (b).

(a)

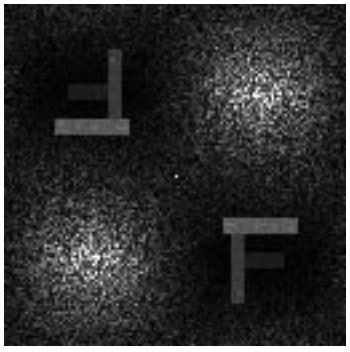

(b)

Fig. 7. Binary hologram generated by error diffusion (a) and its computed reconstruction (b).

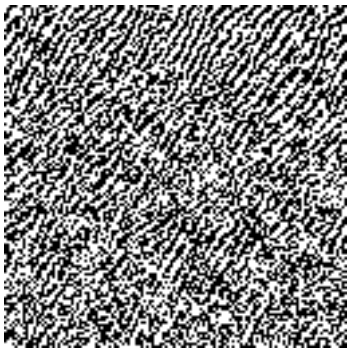

(a)

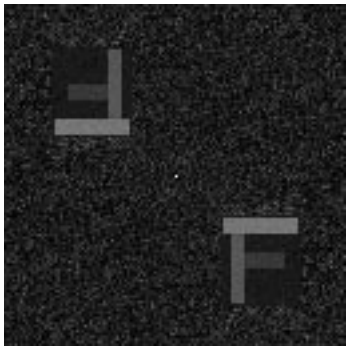

(b)

Fig. 8. Binary hologram generated by direct binary search (a) and its computed reconstruction (b).

(a)

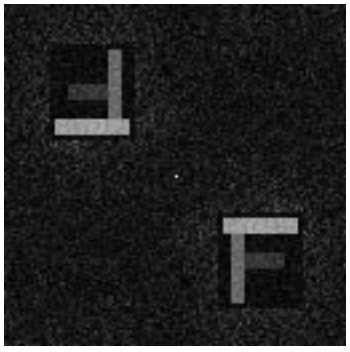

(b)

Fig. 9. Binary hologram generated by iterative stepwise quantization (a) and its computed reconstruction (b).

Fig. 10. The emblem of the University of Mannheim as object.

Fig. 11. Optical reconstruction of the binary hologram generated by iterative stepwise quantization.

Fig. 12. Optical reconstruction of the binary hologram generated by gradual and random binarization (GRB).

Table I. Changes of the MSE in each iteration for the example (letter 'F')

Iteration No. i (S_i)	Number of binarized pixels	MSE at begin of iteration	MSE at end of iteration
1 (S_1=8)	2048	0.05354	0.02586
2 (S_2=4)	4096	0.03573	0.01698
3 (S_3=2)	8192	0.02116	0.01300
4 (S_4=1)	16384	0.01575	0.01420

Table II. Results of simulation of binary holograms generated by different methods and computational complexity of these methods

Methods	MSE (10^{-2})	h (%)	Complexity
Hard clipping	9.78	8.97	O(N)
Error diffusion	5.04	1.09	O(N)
Direct binary search	1.40	3.97	$O(N^{7/4}[\log_2 N]^{3/4})$
Iterative stepwise quantization	2.79	6.45	$O(N\log_2 N)$
Gradual and random binarization	1.80	6.17	$O(N\log_2 N)$

Table III. Calculated MSE, h and measured h' from the reconstruction of binary holograms

Methods	MSE (10^{-2})	h (%)	h' (%)
Iterative stepwise quantization	7.95	6.27	6.81
Gradual and random binarization	3.27	6.05	6.37